




# Copper Nanoparticles Assisted Preservation of Palm Fronds Against Microbes

Vaibhav Arya <sup>1</sup>, Sameena Mehtab <sup>1</sup> , Rahul Patwal <sup>1</sup>, Shiwang Pandey <sup>1</sup>, Mohammad Aziz <sup>1</sup>, Diksha Palariya <sup>1</sup>, M.G.H. Zaidi <sup>1,\*</sup> , Satya Kumar <sup>2</sup>, Shilpi Rawat <sup>2</sup> 

<sup>1</sup> Department of Chemistry, College of Basic Sciences & Humanities, G. B. Pant University of Agriculture and Technology, Pantnagar, Udham Singh Nagar – 263145, Uttarakhand, India; vaibhav.arya02@gmail.com (V.A.); smiitr@gmail.com (S.M.); rahul02patwal@gmail.com (R.P.); pandeyshiwang9897@gmail.com (S.P.); mohammadaziz04@gmail.com (M.A.); palariyadiksha.17@gmail.com (D.P.); mgh\_zaidi@yahoo.com (M.G.H.Z);

<sup>2</sup> Department of Plant Pathology, College of Agriculture, G. B. Pant University of Agriculture and Technology, Pantnagar, Udham Singh Nagar - 263145, Uttarakhand, India; skumar8326@rediffmail.com (S.K.); rawatshilpi19@gmail.com (S.R.);

\* Correspondence: mgh\_zaidi@yahoo.com (M.G.H.Z);

Scopus Author ID 7102180972

Received: 28.08.2023; Accepted: 7.07.2024; Published: 27.08.2024

**Abstract:** The study investigated the synthesis and applications of copper nanoparticles, which are used as a promising material in various sectors, including electronics, machinery, healthcare, agriculture, and energy. Copper nanoparticles exhibit enhanced antibacterial properties compared to traditional medicine, owing to their inherent antimicrobial, antiviral, and anticancer capabilities. L-ascorbic acid (Vitamin C) was employed in the synthesis of copper nanoparticles, serving a dual role as a reducing and capping agent, leading to stable, uniformly dispersed particles, with cupric chloride used as a precursor. Characterization of the copper nanoparticles was accomplished through UV-visible spectroscopy, Fourier transform infrared spectroscopy, and Zeta Potential measurements, elucidating the nanoparticles' optical, molecular, and charge characteristics, respectively. The antimicrobial potential of copper nanoparticles was demonstrated through tests against pathogenic bacteria *Xanthomonas oryzae*, *Bacillus* sp., *Pseudomonas* sp., and *Clostridium* sp. showing superior performance compared to untreated palm fronds. The research highlighted the antimicrobial efficacy of copper nanoparticles, particularly underscoring their potential in wood preservation to combat decay and deterioration caused by microbial infestations.

**Keywords:** copper nanoparticles; *Roystonea regia*; palm fronds; preservation; zeta potential; spectral characterization; antimicrobial behavior.

© 2024 by the authors. This article is an open-access article distributed under the terms and conditions of the Creative Commons Attribution (CC BY) license (<https://creativecommons.org/licenses/by/4.0/>).

## 1. Introduction

Royal palm (*Roystonea regia*), indigenous to South Florida and Cuba, is a popular choice for street or specimen trees due to its ability to bring an orderly yet lavish aesthetic to expansive landscapes. The tree possesses a smooth light-grey trunk that can achieve a diameter of up to 2 feet and rapidly grows to towering heights of between 50 and 70 feet. The tightly overlapping bases of the royal palms' leaves form a smooth, green area, referred to as the "crown shaft", which measures up to 5 feet in height [1]. The crown shaft discarded from royal palm constitutes a kind of agro-waste used for the development of household items, roofing, and temporary partition walls in villages. Under humid environments, palm fronds suffer from microbial invasion within a week, which requires preservation for prolonged applications under changing weather conditions [2].

Preservation of lignocellulosic biomass through the implementation of nanotechnology has received enormous attention over a couple of decades [3]. The creation of novel nanomaterials has become a central area of interest across various research disciplines aimed at contributing to both industrial and technological progress. Nanoparticles (NPs), with their unique physical, chemical, electrical, magnetic, and catalytic properties, have attracted significant attention over decades [4,5]. Copper (Cu), the 8<sup>th</sup> most abundant metallic element in the earth's crust, stands out due to its superior antimicrobial properties [6]. Copper and its compounds have been known for their disinfecting properties, attributed to their antibacterial and antiviral characteristics, for centuries [7]. The high surface-to-volume ratio of copper nanoparticles (CuNPs), akin to other metallic nanoparticles, results in potent antibacterial properties [8].

In contrast to noble metals like gold, silver, or palladium, Cu delivers nanoparticles with a high surface area-to-volume ratio, cost-effective production, effective antibacterial agent, and enhanced catalytic activity. However, their synthesis and maintenance are challenging as they tend to oxidize when exposed to air. To mitigate this, scientists utilize various inert mediums such as Argon and Nitrogen [3-5], as well as reducing, capping, or protective agents to reduce copper into CuNPs [9].

Methods to synthesize CuNPs fall into two main categories: top-down (physical) methods and bottom-up (chemical) methods. The former involves deconstructing the bulk material into nano-sized particles, while the latter involves building nanoparticles using atoms [10]. These methods further branch out into physical, chemical, and biological mechanisms. Physical techniques encompass pulsed laser ablation [11], pulsed wire discharge [12], and mechanical milling [13], while chemical approaches include chemical reduction [14], microemulsion techniques [15], electrochemical [16], microwave-assisted [17], and hydrothermal methods [18]. Chemical reduction stands out as a popular method for synthesizing CuNPs due to its simplicity and affordability. This technique utilizes various reducing and stabilizing agents to produce CuNPs with controlled size and shape.

In the present study, a facile method was utilized for the synthesis of CuNPs using ascorbic acid as a reducing agent. Ascorbic acid served a dual purpose in the synthesis process, acting as a reducing and capping agent. Its reducing properties facilitated the conversion of copper ions to CuNPs, while its capping abilities contributed to stabilizing the formed nanoparticles and preventing their agglomeration [19]. CuNPs were used to preserve palm fronds (*Roystonea regia*) for potential application in the development of microbe-resistant domestic articles such as mats, particle boards, and cardboards [2]. The antibacterial potential of the preserved royal palm fronds (RPF) was further investigated against four bacterial strains: *Xanthomonas oryzae*, *Bacillus* sp., *Pseudomonas* sp., and *Clostridium* sp.

## 2. Materials and Methods

### 2.1. Experimental.

Copper (II) chloride  $\text{CuCl}_2 \cdot 2\text{H}_2\text{O}$  and L-Ascorbic Acid (>99%) were procured by R. K. Scientific and Chemicals, India. CuNPs were synthesized through the chemical reduction method and prepared by mixing the solutions of  $\text{CuCl}_2 \cdot 2\text{H}_2\text{O}$  (0.01 molar, 50 mL) and L-ascorbic acid (0.5 molar, 5 mL) under magnetic stirring (500 rpm at 90°C) till the solution's color transitioned from yellow to dark brown to black. The product was left undisturbed for 12 weeks [20].

## 2.2. Characterization.

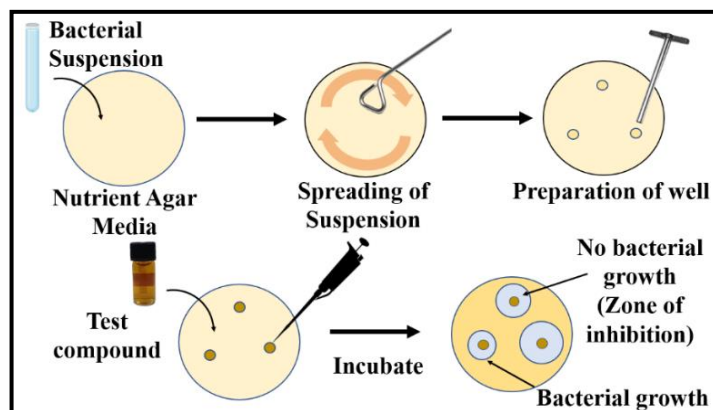
The distribution range of the synthesized particles from the samples was obtained using dynamic light scattering (DLS) and a Malvern ZEN3600 ZetaSizer at 24.9°C. Fourier transform infrared spectroscopy (FTIR) spectra were recorded on Bruker Alpha II spectrophotometer. UV-visible spectroscopy (UV-Vis) spectra were recorded on Hitachi U-2900 spectrophotometer.

## 2.3. Antibacterial assay.

The antimicrobial assay was conducted against bacteria belonging to the genera *Bacillus*, *Clostridium* (gram-positive), *Pseudomonas*, and *Xanthomonas oryzae* (gram-negative) as per the standard test method [21]. The bacteria isolated from the rhizosphere of the palm tree were procured and reisolated by streaking on Nutrient Agar (NA) media plates, incubated at 37°C for 24-48 hrs. The identification was performed by applying the gram staining test and observing the colonies under a 100X Olympus binocular compound microscope. Three wells, each of 0.5 cm diameter, equidistance to each other, were inscribed in freshly inoculated NA plate streaked with bacterial colony. The antibacterial properties of CuNPs were tested using the good diffusion method, where the CuNPs were added into the wells at concentrations (conc.) adjusted at 0.5, 1.0, 2.0, and 3.0 ppm in different NA plates. The plates were incubated at 26-28°C till the appearance of bacterial zones (Scheme 1), along with control plates (without CuNPs). The percentage inhibition, as mentioned in Figure 1 was calculated by the given formula:

$$\text{Percent Inhibition} = \frac{(C - T)}{C} \times 100$$

where 'C' is the radial growth in the control treatment and 'T' is the radial growth in treatment treated with CuNPs.



**Scheme 1.** The diagrammatic procedure of antibacterial assay.

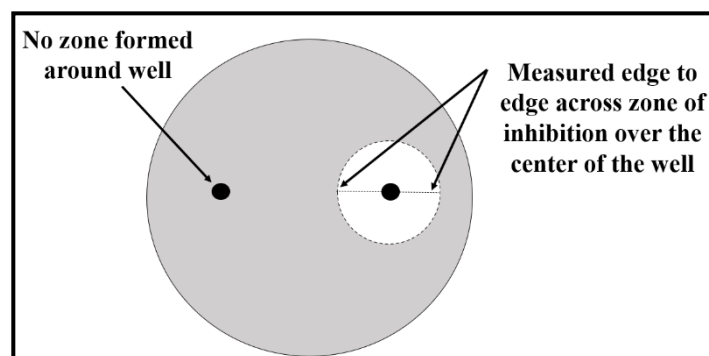
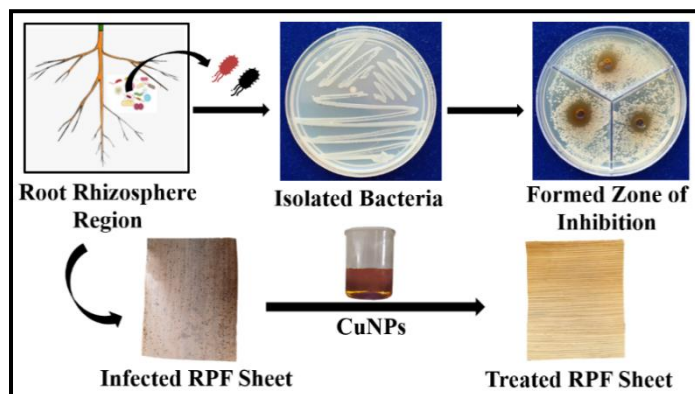


**Figure 1.** Calculation of zone of inhibition.

#### 2.4. Treatment of the royal palm frond (RPF) sheets with CuNPs.

A systematic study was conducted to preserve RPF sheets. The conc. of CuNPs showing inhibition to bacterial colonies in the NA media were selected. The infected RPF sheets were first surface-sterilized with HgCl<sub>2</sub>, followed by rinsing with distilled water. The sheets were immersed in a prepared solution of CuNPs of desired conc. For 17 hrs (Scheme 2), with subsequent observations on bacterial growth and zone of inhibition formation after 4 days.



**Scheme 2.** Preservation of RPF with CuNPs and their screening against the test bacteria.

### 3. Results and Discussion

#### 3.1. Characterization of CuNPs.

The CuNPs synthesized through the chemical reduction method were characterized using the UV-Vis spectra, FTIR, and Zeta sizer. UV-Vis spectral analysis indicated that the CuNPs exhibited a surface plasmon resonance absorption band at 570 nm in Figure 2(a). It has been reported that this excitation of plasmon resonance or inter-band transition indicates the metallic characteristics of CuNPs, which is characteristic of CuNPs and confirms the formation of metal NPs [22]. In addition, the spectra showed no other peaks, attesting to the purity of the synthesized CuNPs. Further characterization performed using Zeta sizer analysis revealed that the size of CuNPs is ~90nm Figure 2(c). The interaction between L-ascorbic acid and CuNPs changed the mixture's composition, which was further studied using FTIR Spectroscopy [23]. The spectra identified peaks at 3432 cm<sup>-1</sup>, 2375 cm<sup>-1</sup>, 2073 cm<sup>-1</sup>, and 1637 cm<sup>-1</sup>; these peaks were associated with the enol hydroxyl group, scissor-bending vibration of molecular water, an asymmetric stretch of acid, and C-H deformations of -CH<sub>2</sub> or -CH<sub>3</sub> groups [20] Figure 2(b). Overall, this comprehensive characterization process confirms the successful synthesis of CuNPs and their interaction with L-ascorbic acid. Further comparing the FTIR spectra of pristine CuCl<sub>2</sub> with the FTIR spectra of L-ascorbic acid stabilized CuNPs reveals significant differences in observed peaks and their implications. The FTIR spectra of pristine CuCl<sub>2</sub> exhibit peaks associated with carboxyl or carbonyl groups, indicating chemical transformations during the reduction process. The shift in peak positions further suggests the formation of metal carbonyl groups due to the stabilization of CuNPs by the -COO- group [24]. These findings highlight the distinct chemical pathways involved in the synthesis of CuNPs and emphasize the role of stabilizing agents in NPs formation. This comprehensive characterization confirms the successful synthesis of CuNPs, with evidence supporting their purity, size uniformity, and interaction with L-ascorbic acid, compared with pristine CuCl<sub>2</sub>.

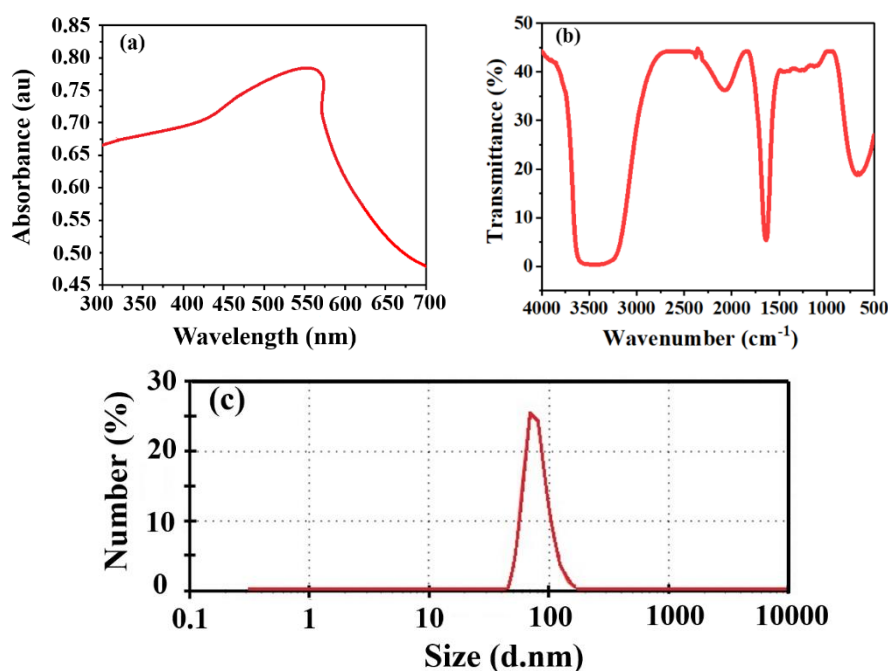


**Figure 2.** Characterization of CuNPs as follows: (a) UV-Vis; (b) FTIR; (c) Zeta potential.

### 3.2. Morphological identification of bacterial species.

The bacterial colonies of the four major generals were morphologically identified and categorized as per the observations made in Table 1 and Figure 3.

**Table 1.** Morphological characteristics of bacterial colonies isolated.

| S. No. | Bacteria identified    | Gram staining result | Shape observed | Characteristic features observed | Colonies on NA plate   |
|--------|------------------------|----------------------|----------------|----------------------------------|--|
| 1      | <i>X. oryzae</i>       | -ve                  | Rod-shaped     | Single polar flagellum           | Yellow pigmentation.   |
| 2      | <i>Bacillus</i> sp.    | +ve                  | Rod-shaped     | Endospores formation             | Large irregular.   |
| 3      | <i>Pseudomonas</i> sp. | -ve                  | Rod-shaped     | Endospores formation             | Circular and smooth.   |
| 4      | <i>Clostridium</i> sp. | +ve                  | Rod-shaped     | -                                | Variety of colonies: round, smooth, irregular, and/or rhizoid. |

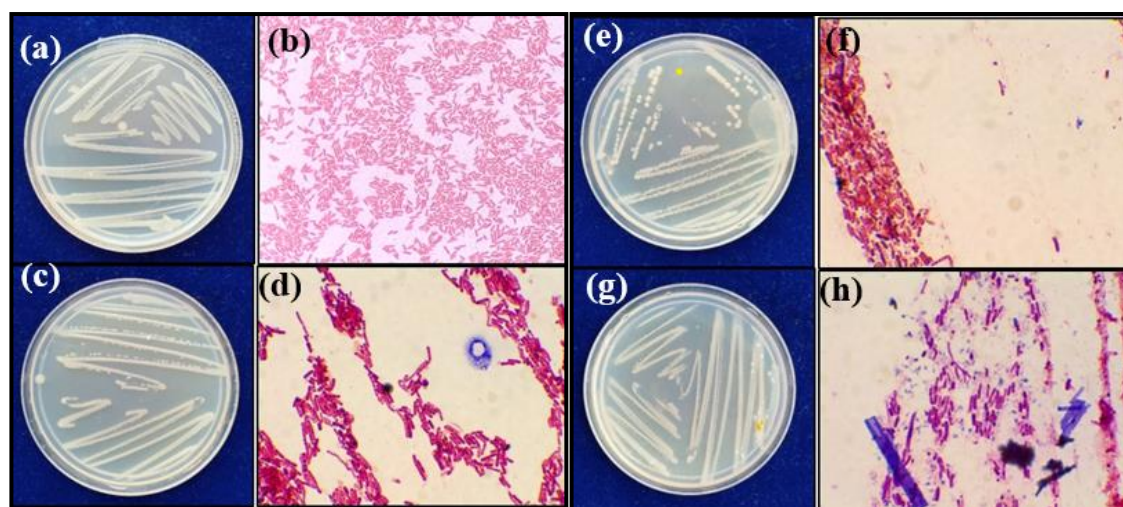


**Figure 3.** Characterization of the bacterial colonies. (a) *X. oryzae*; (b) microscopic view of *X. oryzae*; (c) *Clostridium* sp.; (d) microscopic view of *Clostridium* sp.; (e) *Pseudomonas* sp.; (f) microscopic view of *Pseudomonas* sp.; (g) *Bacillus* sp.; (h) microscopic view of *Bacillus* sp.

### 3.3. Antibacterial activity.

Among the test bacteria, as mentioned in Figure 4, *X. oryzae* demonstrated the highest susceptibility to CuNPs, showing a zone of inhibition (ZI) of 1.5 mm with a percent zone of inhibition (PZI) of 43% at a concentration of 3 ppm. This was significantly higher than the results seen with other bacteria. It continued to exhibit a substantial inhibitory effect even at lower concentrations of 2 and 1 ppm, with ZI of 1.4 mm and 1.2 mm and PZI of 35% and 31%, respectively. *Clostridium* sp. showed a ZI of 1.2 mm and 1.0 mm and PZI of 38% at 3 ppm, and at concentrations of 2 and 1 ppm, the PZI measured 31% and 25%, respectively. In the case of *Pseudomonas* sp., a 1.4 mm ZI was observed at 3 ppm with a PZI of 35% and ZI of 1.2 mm and 1.0 mm were observed with PZI measuring 30% and 25% at 2 and 1 ppm, respectively. For *Bacillus* sp., a ZI of 1.2 mm was recorded at 3 ppm with a PZI of 32%, and ZIs of 1.0 mm and 0.7 mm were observed with PZI measuring 26% and 19% at 2 and 1 ppm, respectively. According to Table 2, all four bacterial species exhibited significant susceptibility to the CuNPs solution, as evidenced by the ZI at various concentrations, with zones reducing as CuNPs concentration decreased.

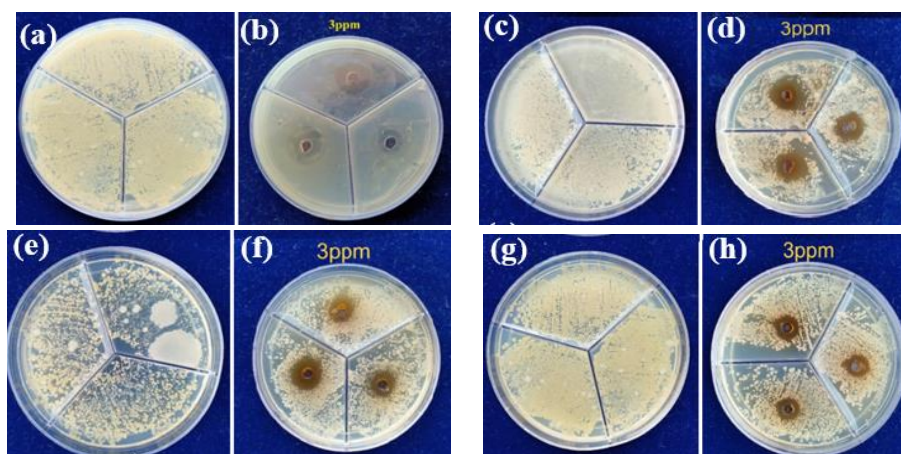


**Figure 4.** Photos of NA plates inoculated with CuNPs at 3 ppm conc. (a) *X. oryzae* (control); (b) formation of ZI; (c) *Clostridium* sp. (control); (d) formation of ZI; (e) *Pseudomonas* sp. (Control); (f) formation of ZI; (g) *Bacillus* sp. (control); (h) formation of ZI.

**Table 2.** Antibacterial analysis of CuNPs at different concentrations. Data analyzed with two-way analysis, found to be significant at  $p < 0.05$ , values within a column followed by a single letter (a, b, c, and d) show significant varietal difference by Tukey's test.

| Solution concentration(ppm) | Mean/ZI (%)                 |                             |                             |                            |             |
|-----------------------------|-----------------------------|-----------------------------|-----------------------------|----------------------------|-------------|
|                             | <i>Pseudomonas</i> sp.      | <i>Clostridium</i> sp.      | <i>Bacillus</i> sp.         | <i>Xanthomonas</i> sp.     | Control(cm) |
| 0.5                         | 0.7 <sup>cd</sup> (17)      | 0.8 <sup>bcd</sup> (20)     | 0.5666 <sup>d</sup> (14)    | 0.7833 <sup>bcd</sup> (19) | -           |
| 1                           | 1.0333 <sup>abcd</sup> (25) | 1.0333 <sup>abcd</sup> (25) | 0.7833 <sup>bcd</sup> (19)  | 1.2666 <sup>abc</sup> (31) | -           |
| 2                           | 1.2 <sup>abcd</sup> (30)    | 1.2666 <sup>abc</sup> (31)  | 1.0666 <sup>abcd</sup> (26) | 1.4166 <sup>ab</sup> (35)  | -           |
| 3                           | 1.4 <sup>ab</sup> (35)      | 1.55 <sup>a</sup> (38)      | 1.2 <sup>abcd</sup> (32)    | 1.5833 <sup>a</sup> (43)   | -           |

SEm: ±0.062, C.D.: 0.180 and SEd: ±0.088

\*SEm: Standard error of the mean; C.D.: Critical difference; SEd: Standard error of the difference between two means.

### 3.4. Statistical analysis and discussion.

As per Table 2, a two-way ANOVA analysis was performed (significant at  $p < 0.05$ ), which supported the conclusion that CuNPs display considerable antibacterial activity against the tested bacteria. The varietal difference highlighted by Tukey's test indicates the different levels of susceptibility amongst the bacterial strains, with *X. oryzae* being the most sensitive. Upon observation

of infected/contaminated RPF sheets immersed in CuNPs solutions for 4 days, a 3 ppm concentration of CuNPs was the most effective, with no bacterial growth on the sheets, with 1 and 2 ppm solutions showed slow growth, and no growth inhibition was observed in the 0.5 ppm solution. Our current results align with research by Chompunut *et al.* [25], Murthy *et al.* [26], and Rajesh *et al.* [27], all of whom elucidated the impact of *Bacillus* sp. bacterial growth on ZI. They revealed respective ZI of 15 mm, 14.2 mm, and 8 mm for different positive strains of *Bacillus* sp. This indicates the potential antimicrobial properties of *Bacillus* sp. In the present experiment, using CuNPs yielded a 13 mm ZI against *Bacillus* sp. These findings suggest that our prepared CuNPs could be comparably effective as an antimicrobial agent. These results further substantiate the potential use of CuNPs as a viable alternative in microbial control.

#### 4. Conclusions

In conclusion, the research findings provide valuable insights into the characteristics of CuNPs and their antibacterial application in the domain of wood preservation. The successful synthesis of CuNPs using  $\text{CuCl}_2 \cdot 2\text{H}_2\text{O}$  and L-ascorbic acid was demonstrated, and their characteristics were comprehensively evaluated through UV-Vis absorption spectra, Zeta sizer analysis, and FTIR spectroscopy. Moreover, the examination of the prepared CuNPs revealed interesting observations. The synthesized CuNPs exhibited potent antibacterial properties against four bacterial strains, with *X. oryzae* demonstrating the highest sensitivity. The study showcased CuNPs as potential antimicrobial agents against bacterial infections at appropriate concentrations. In the context of wood preservation, these findings hold significant relevance. The antimicrobial efficacy of CuNPs could offer an innovative and effective strategy to mitigate such damage, enhancing the longevity of wood products. Overall, this research provides important information about the composition and characteristics of CuNPs and their resulting antibacterial activity with respect to wood preservation. The research sets the foundation for the integration of CuNPs into wood preservation techniques as a sustainable and efficient strategy to impart protection against harmful bacteria. In conclusion, the study opens a new avenue in the field of wood preservation, advocating for the use of CuNPs as a potential antimicrobial agent. Further studies can build upon these findings to explore the practical implications and potential uses of CuNPs in various fields.

#### Funding

This research received no external funding.

#### Acknowledgments

The authors express their gratitude towards the Departments of Chemistry and Plant Pathology, G.B. Pant University of Agriculture and Technology, Pantnagar, with special mentions to Dr. M.G.H. Zaidi and Dr. Sameena Mehtab. Our sincere thanks also go to Dr. Satya Kumar and Dr. Shilpi Rawat from the Department of Plant Pathology for their invaluable advice and provision of testing facilities.

#### Conflicts of interests

There is no conflict of interest between authors.

## References

1. Munir, M.U.; Saeed, M.A.; Masood, Z.; Aslam, N.; Farooq, M. Physicochemical, phytochemical evaluation and pharmacological investigation of *Roystonea regia*. *Res. J. Pharm. Technol.* **2023**, *16*, 1738-1742, <https://doi.org/10.52711/0974-360X.2023.00286>.
2. Patwal, R.; Arya, V.; Aziz, M.; Pandey, S.; Siddiqui, T.I.; Mehtab, S.; Zaidi, M.G.H. Modification in thermal and electrical characteristics of royal palm frond (*Roystonea regia*) through blending with high-density polyethylene. *Bulg. Chem. Commun.* **2023**, *55*, 126-130.
3. Ghosh, P.; Deepshikha, K.; Kumar, R.R.; Chaturvedi, V.; Verma, P. Recent advances of nanotechnology in ameliorating bioenergy production: A comprehensive review. *Sustain. Chem. Pharm.* **2024**, *37*, 101392, <https://doi.org/10.1016/j.scp.2023.101392>.
4. Awogbemi, O.; Von Kallon, D.V. Recent advances in the application of nanomaterials for improved biodiesel, biogas, biohydrogen, and bioethanol production. *Fuel* **2024**, *358*, 130261, <https://doi.org/10.1016/j.fuel.2023.130261>.
5. Díez, A.G.; Rincón-Iglesias, M.; Lanceros-Méndez, S.; Reguera, J.; Lizundia, E. Multicomponent magnetic nanoparticle engineering: the role of structure-property relationship in advanced applications. *Mater. Today Chem.* **2022**, *26*, 101220, <https://doi.org/10.1016/j.mtchem.2022.101220>.
6. Aragón-Muriel, A.; Reyes-Márquez, V.; Cañavera-Buelvas, F.; Parra-Unda, J.R.; Cuenú-Cabezas, F.; Polo-Cerón, D.; Colorado-Peralta, R.; Suárez-Moreno, G.V.; Aguilar-Castillo, B.A.; Morales-Morales, D. Pincer Complexes Derived from Tridentate Schiff Bases for Their Use as Antimicrobial Metallopharmaceuticals. *Inorganics* **2022**, *10*, 134, <https://doi.org/10.3390/inorganics10090134>.
7. Tortella, G.R.; Pieretti, J.C.; Rubilar, O.; Fernández-Baldo, M.; Benavides-Mendoza, A.; Diez, M.C.; Seabra, A.B. Silver, copper and copper oxide nanoparticles in the fight against human viruses: progress and perspectives. *Crit. Rev. Biotechnol.* **2022**, *42*, 431-449, <https://doi.org/10.1080/07388551.2021.1939260>.
8. Nieto-Maldonado, A.; Bustos-Guadarrama, S.; Espinoza-Gomez, H.; Z. Flores-López, L.; Ramirez-Acosta, K.; Alonso-Núñez, G.; Cadena-Nava, R.D. Green synthesis of copper nanoparticles using different plant extracts and their antibacterial activity. *J. Environ. Chem. Eng.* **2022**, *10*, 107130, <https://doi.org/10.1016/j.jece.2022.107130>.
9. Humphreys Salas, Z.; Martínez Ávila, A.F.; Hernández Orozco, M.M.; Elizalde Peña, E.A.; Palma Tirado, L.; Baldenegro Pérez, L.A.; Padilla Vaca, F.; Luna-Bárceñas, G.; España Sánchez, B.L. Green synthesis of copper nanoparticles and their formulation into face masks: An antibacterial study. *Polym. Compos.* **2023**, *44*, 907-916, <https://doi.org/10.1002/pc.27142>.
10. Tran, T.V.; Nguyen, D.T.C.; Kumar, P.S.; Din, A.T.M.; Jalil, A.A.; Vo, D.-V.N. Green synthesis of ZrO<sub>2</sub> nanoparticles and nanocomposites for biomedical and environmental applications: a review. *Environ. Chem. Lett.* **2022**, *20*, 1309-1331, <https://doi.org/10.1007/s10311-021-01367-9>.
11. Kumari, S.; Raturi, S.; Kulshrestha, S.; Chauhan, K.; Dhingra, S.; Andrés, K.; Thu, K.; Khargotra, R.; Singh, T. A comprehensive review on various techniques used for synthesizing nanoparticles. *J. Mater. Res. Technol.* **2023**, *27*, 1739-1763, <https://doi.org/10.1016/j.jmrt.2023.09.291>.
12. Li, C.; Han, R.; Bai, J.; Cao, Y.; Yuan, W.; Wu, J.; Li, P.; Chen, X. One-step synthesis of structural-controlled metal-graphene nanocomposites via flash atomization and plasma-assisted reactions of electrical explosion. *Carbon* **2023**, *213*, 118296, <https://doi.org/10.1016/j.carbon.2023.118296>.
13. Harish, V.; Ansari, M.M.; Tewari, D.; Yadav, A.B.; Sharma, N.; Bawarig, S.; García-Betancourt, M.-L.; Karatutlu, A.; Bechelany, M.; Barhoum, A. Cutting-edge advances in tailoring size, shape, and functionality of nanoparticles and nanostructures: A review. *J. Taiwan Inst. Chem. Eng.* **2023**, *149*, 105010, <https://doi.org/10.1016/j.jtice.2023.105010>.
14. Beheshti, A.K.; Rezaei, M.; Alavi, S.M.; Akbari, E.; Varbar, M. Cobalt nanoparticle synthesis through the mechanochemical and chemical reduction method as a highly active and reusable catalyst for H<sub>2</sub> production via sodium borohydride hydrolysis process. *Int. J. Hydrog. Energy* **2024**, *51*, 661-670, <https://doi.org/10.1016/j.ijhydene.2023.10.168>.
15. Salabat, A.; Mirhoseini, F. Polymer-based nanocomposites fabricated by microemulsion method. *Polym. Compos.* **2022**, *43*, 1282-1294, <https://doi.org/10.1002/pc.26504>.
16. Sun, X.; Cheng, H.; Li, M.; Chen, J.; Li, D.; Liu, B.; Jiang, Y.; Duan, X.; Hu, J. Collision electrochemical synthesis of metal nanoparticles using electrons as green reducing agent. *ACS Appl. Mater.* **2022**, *14*, 57189-57196, <https://doi.org/10.1021/acsami.2c18114>.
17. Takai, T.; Shibatani, A.; Asakuma, Y.; Saptorio, A.; Phan, C. Microwave-assisted nanoparticle synthesis enhanced with addition of surfactant. *Chem. Eng. Res. Des.* **2022**, *182*, 714-718, <https://doi.org/10.1016/j.cherd.2022.04.035>.



18. Asjadi, F.; Yaghoobi, M. Characterization and dye removal capacity of green hydrothermal synthesized ZnO nanoparticles. *Ceram. Int.* **2022**, *48*, 27027-27038, <https://doi.org/10.1016/j.ceramint.2022.06.015>.
19. Chaerun, S.K.; Prabowo, B.A.; Winarko, R. Bionanotechnology: The formation of copper nanoparticles assisted by biological agents and their applications as antimicrobial and antiviral agents. *Environ. Nanotechnol. Monit. Manag.* **2022**, *18*, 100703, <https://doi.org/10.1016/j.enmm.2022.100703>.
20. Umer, A.; Naveed, S.; Ramzan, N.; Rafique, M.S.; Imran, M. A green method for the synthesis of Copper Nanoparticles using L-ascorbic acid. *Matéria(Rio de janeiro)* **2014**, *19*, 197-203, <https://doi.org/10.1590/S1517-70762014000300002>.
21. Varaldo, P.E. Antimicrobial resistance and susceptibility testing: an evergreen topic. *J. Antimicrob. Chemother.* **2002**, *50*, 1-4, <https://doi.org/10.1093/jac/dkf093>.
22. Shah, A.T.; Ahmad, S.; Kashif, M.; Khan, M.F.; Shahzad, K.; Tabassum, S.; Mujahid, A. In situ synthesis of copper nanoparticles on SBA-16 silica spheres. *Arab. J. Chem.* **2016**, *9*, 537-541, <https://doi.org/10.1016/j.arabjc.2014.02.013>.
23. Soltau Missio Pinheiro, L.D.; Sentena, N.Z.; Sangoi, G.G.; Vizzotto, B.S.; de Oliveira Pinto, E.; Pavoski, G.; Romano Espinosa, D.C.; Machado, A.K.; Leonardo da Silva, W. Copper nanoparticles from acid ascorbic: Biosynthesis, characterization, *in vitro* safety profile and antimicrobial activity. *Mater. Chem. Phys.* **2023**, *307*, 128110, <https://doi.org/10.1016/j.matchemphys.2023.128110>.
24. Karikalan, N. Synthesis and characterization of copper nanoparticles and evaluation of antibacterial activity. *Rasayan J. Chem.* **2018**, *11*, 1451-1457, <https://doi.org/10.31788/RJC.2018.1143068>.
25. Chompunut, L.; Wanaporn, T.; Anupong, W.; Narayanan, M.; Alshiekheid, M.; Sabour, A.; Karuppusamy, I.; Lan Chi, N.T.; Shanmuganathan, R. Synthesis of copper nanoparticles from the aqueous extract of *Cynodon dactylon* and evaluation of its antimicrobial and photocatalytic properties. *Food Chem. Toxicol.* **2022**, *166*, 113245, <https://doi.org/10.1016/j.fct.2022.113245>.
26. Murthy, H.C.A.; Desalegn, T.; Kassa, M.; Abebe, B.; Assefa, T. Synthesis of Green Copper Nanoparticles Using Medicinal Plant *Hagenia abyssinica*(Brace) JF. Gmel. Leaf Extract: Antimicrobial Properties. *J. Nanomater.* **2020**, *2020*, 3924081, <https://doi.org/10.1155/2020/3924081>.
27. Rajesh, K.M.; Ajitha, B.; Reddy, Y.A.K.; Suneetha, Y.; Reddy, P.S. Assisted green synthesis of copper nanoparticles using *Syzygium aromaticum* bud extract: Physical, optical and antimicrobial properties. *Optik* **2018**, *154*, 593-600, <https://doi.org/10.1016/j.ijleo.2017.10.074>.